

so as to be valid for a large region of mass numbers.

ACKNOWLEDGMENTS

The authors wish to thank S. A. Drentje and Tj. Klootsema for making the implanted source and F. Th. ten Broek for making the ZnTe source and the absorber used in the experiment. This work was done as part of the research program of the

“Stichting voor Fundamenteel Onderzoek der Materie” with financial support from the “Nederlandse Organisatie voor Zuiver Wetenschappelijk Onderzoek.” One of the authors (N.S.W.) would like to express his gratitude to the South African Council for Scientific and Industrial Research for financial support, to Professor H. de Waard for inviting him to Groningen, and to the staff of the Natuurkundig Laboratorium for their hospitality.

*On leave from the University of the North, P.O. Sovenga, Via Pietersburg, South Africa.

¹Nucl. Data **A5**, 498 (1969).

²V. S. Shirley, in *Hyperfine Interactions in Excited Nuclei*, edited by G. Goldring and R. Kalish (Gordon and Breach, London, 1971), Vol. IV, p. 1255.

³P. N. Tandon, S. H. Devare, and H. G. Devare, in *Proceedings of the International Congress on Nuclear Physics, Paris, 1964*, edited by P. Gugenberger (Centre National de la Recherche Scientifique, Paris, 1965), Vol. II, p. 56.

⁴Å. G. Svensson, R. W. Sommerfeldt, L.-O. Norlin, and P. N. Tandon, Nucl. Phys. **A95**, 653 (1967).

⁵L. S. Kisslinger and R. A. Sorensen, Rev. Mod. Phys. **35**, 853 (1963).

⁶G. M. Kalvius, L. D. Oppliger, and S. L. Ruby, Phys.

Letters **18**, 241 (1965).

⁷H. de Waard and S. A. Drentje, Phys. Letters **20**, 38 (1966).

⁸M. Pasternak, Phys. Letters **31A**, 215 (1970).

⁹H. de Waard, S. R. Reintsema, and M. Pasternak, Phys. Letters **33B**, 413 (1970).

¹⁰E. Kankeleit, Rev. Sci. Instr. **35**, 194 (1964).

¹¹H. de Waard, Rev. Sci. Instr. **36**, 1728 (1965).

¹²G. J. Perlow, in *Chemical Applications of Mössbauer Spectroscopy*, edited by V. I. Goldanskii and R. H. Herber (Academic, New York, 1968), p. 418.

¹³J. S. Geiger, R. L. Graham, I. Bergström, and F. Brown, Nucl. Phys. **68**, 352 (1965).

¹⁴S. R. Reintsema, private communication, including the positive sign of the field.

¹⁵B. Castel, Can. J. Phys. **46**, 2571 (1968).

Optical-Model Analysis of Proton Elastic Scattering by ^{208}Pb from 8 to 14 MeV*

T. Mo and R. H. Davis

Department of Physics, The Florida State University, Tallahassee, Florida 32306

(Received 10 January 1972)

The uniqueness and energy dependence of optical-model parameters which describe the $^{208}\text{Pb}(p,p)^{208}\text{Pb}$ scattering reaction have been studied in the bombarding range 8 to 14 MeV. In the analysis of data with a 3% error two discretely ambiguous well depths with mean values of 35 and 55 MeV are found which yield comparably good fits. The imaginary well depth is approximately 4 MeV for both. To select one well depth, a 1% measurement was made at the energy ($E_p = 7.6$ MeV) at which the difference between the two computed cross sections at backward angles is maximized, a difference of approximately 3%. These measurements select the 55-MeV well depth consistent with the number of occupied states in ^{208}Pb . The spin-orbit term is undetermined in this study, since the values of the imaginary potential render the analysis insensitive to it.

I. INTRODUCTION

Elastic scattering of protons by ^{208}Pb below 40 MeV has been measured previously at two discrete energies,^{1,2} 17 and 30 MeV. In several isobaric-analog-state investigations³⁻⁵ protons have been scattered by ^{208}Pb in the bombarding energy range of 14–22 MeV. Below $E_p = 14$ MeV, no measurements have been reported.

No strong anomalies are expected in the excitation curves below 14-MeV proton energy; the lowest isobaric analog state is at 14.95 MeV. On the other hand, the (p, n) reaction is open, and the density of states in the compound system is high. Optical-model analysis of data for $E_p = 8$ to 14 MeV is not hampered by resolvable resonances or the difficulties of making compound elastic scattering estimates. The technique^{6,7} of scattering in the

vicinity of the Coulomb barrier to remove discrete ambiguities in the optical model is applicable. Here it is used to discriminate between two real well depths with mean values of 35 and 55 MeV, selecting the latter.

The energy dependencies⁸ of the real and imaginary well depths have been determined for $E_p = 8$ to 14. The fits to the data were insensitive to the value of the spin-orbit term, consistent with the study by Greenlees *et al.*⁹ While the values of W , the imaginary part of the potential, are small compared with the oscillator spacing (~ 20 MeV), they

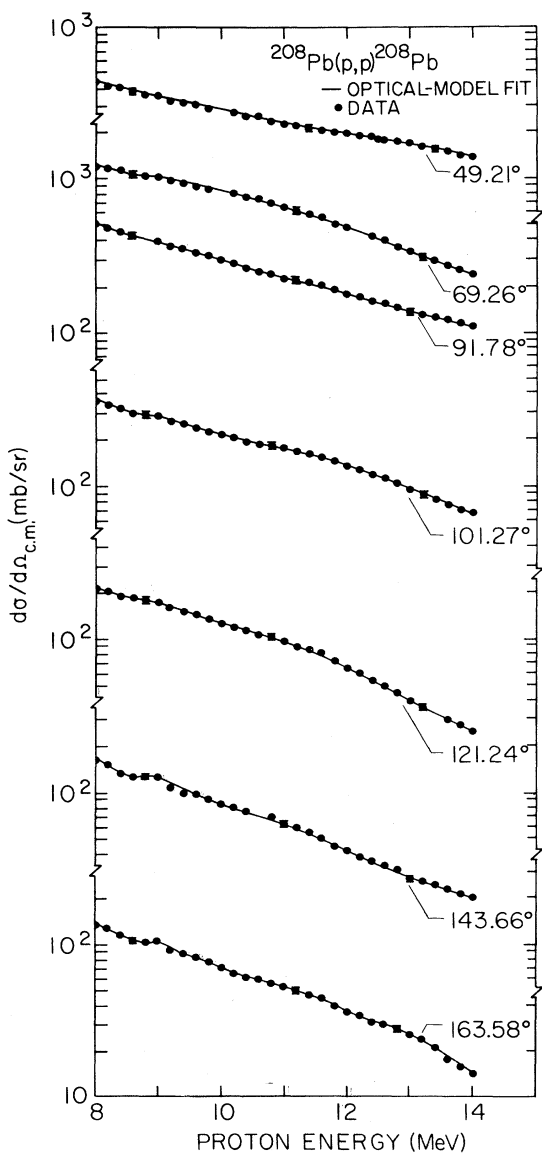


FIG. 1. Excitation functions. The solid curves are the best fits obtained using the optical-model parameters given in Table I and Fig. 3. The c.m. angles are labeled on the right side.

are comparable to the splitting due to spin-orbit coupling. Consequently, acceptable values of the spin-orbit coupling parameter have negligible effect on the calculated cross sections.

II. EXPERIMENTAL PROCEDURE

Proton beams from the super FN tandem¹⁰ were bent and focused at the target position of an 18-in.-diam scattering chamber.¹¹ Eight silicon surface-barrier detectors mounted on a rotatable detector ring mount were used in these measurements. The range of angles covered by this ring was 25 to 165° in the laboratory system. In addition, a monitor counter was fixed at 20°.

The excitation functions were measured in 100- to 200-keV steps, and at each of these energies a 32-point angular distribution was obtained with four ring settings. The target was a self-supporting foil of ²⁰⁸Pb (enriched to 99.9%) with effective thickness 1.2 mg/cm² which corresponds to 40–50-

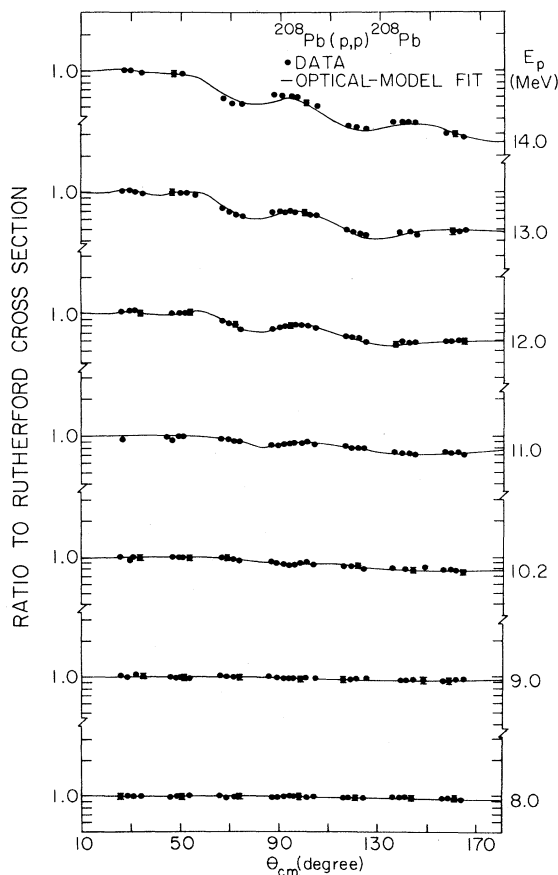


FIG. 2. Angular distribution at different bombarding energies. The solid curves are the best fits. The best-fit parameters are given in Table I (see also Fig. 3) and explained in the text.

keV energy loss over the proton bombarding energy range.

The detector pulses were sorted by a TMC 4096-channel analyzer and the digitized information was transmitted to an EMR 6130 computer. Elastically scattered proton peak yields were extracted from each spectrum with a light pen and stored on a magnetic tape which also recorded the live-time¹² of the analyzer and other run parameters.

Absolute differential cross sections were determined at $E_p = 7.0$ MeV by assuming the cross sections equal to the Rutherford scattering at all angles. All data at other energies were normalized to this measurement. For the radius chosen, the classical Coulomb-barrier height is 11 MeV.

Statistical errors in the peak yields were typically 1–2% in most of the runs. The errors in the absolute values of cross sections were estimated to be 3–4% over all angles. Seven of the excitation curves and angular distributions are shown in Figs. 1 and 2. The dots are the experimental data and the solid curves are optical-model fits which are discussed in the following section. In the experimental excitation functions (Fig. 1), a brief rise in cross section appears at all angles at about $E_p \sim 9$ MeV, where the cross sections start to deviate from Rutherford scattering. A similar phenomenon was observed in the elastic scattering of α particles from ^{208}Pb by Kerlee, Blair, and Farwell.¹³

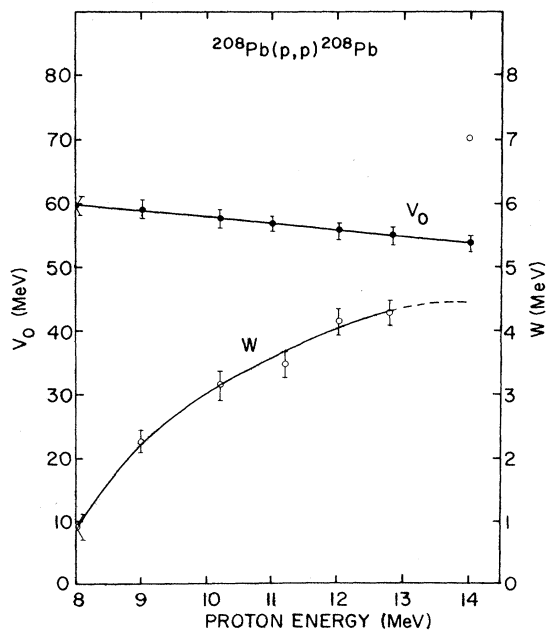


FIG. 3. The energy dependence of the optical-model potential strengths obtained from the best fits to the data. The dashed part on the W curve and the "error bars" on both curves are explained in the text.

After determining the set of discretely ambiguous well depths, as discussed in the next section, an additional angular-distribution measurement was made at $E_p = 7.6$ MeV with a thin target (~ 5 keV) for which the error relative to Rutherford scattering was less than 1%. The purpose of this measurement was to select one of the two comparably good well depths at the energy for which the difference in the computed results was maximized (see Fig. 6).

III. ANALYSIS

The optical-model potential used in the present analysis was

$$V(r) = -V_0 f(r, R_r, a_r) - iW_0 f(r, R_i, a_i) - \frac{V_{s0}}{a_{s0}\gamma} e^{(r-R_{s0})/a_{s0}} f^2(r, R_{s0}, a_{s0}) 2\mathbf{I} \cdot \mathbf{S} + V_C(r), \quad (1)$$

where

$$f(r, R, a) = [1 + e^{(r-R)/a}]^{-1}$$

and

$$V_C(r) = \begin{cases} \frac{Z_p Z_t e^2}{2R_C} \left[3 - \left(\frac{r}{R_C} \right)^2 \right], & r \leq R_C \\ \frac{Z_p Z_t e^2}{r}, & r > R_C. \end{cases}$$

The radius R_C is that of a uniformly charged sphere defined by $R_C = 1.25A^{1/3}$ F, and $Z_p Z_t$ the product of the projectile and the target atomic numbers.

The optical-model parameter search was performed by a CDC 6400 computer. The best-fit criterion for each angular distribution is the minimization of the quantities

$$\chi^2 = \frac{1}{N} \sum_{i=1}^n \left[\frac{\sigma_e(\theta_i) - \sigma_c(\theta_i)}{\Delta\sigma(\theta_i)} \right]^2, \quad (2)$$

where N is the number of data points, $\sigma_e(\theta_i)$ the experimental cross section, $\sigma_c(\theta_i)$ the calculated cross section, and $\Delta\sigma(\theta_i)$ the error assigned to the experimental cross section at the c.m. angle θ_i .

The radius parameters were kept fixed at $R_C = R_r = R_i = 7.5$ F, for which $r_0 = 1.25$ F in $R = r_0 A^{1/3}$. This is in agreement with electron scattering work.¹⁴ The values of R_C , R , and R' are not necessarily the same, but because of continuous (type II)⁷ ambiguities, differences are accommodated here by adjustment of other parameters. Similarly, the diffusenesses of parameters were kept constant at $a_r = a_i = 0.65$ F.

The data for the present analysis cover the energy range 8 to 14 MeV, within which parameter

searches were performed at 1-MeV intervals. Since the optical-potential strengths V_0 and W_0 vary smoothly as a function of the bombarding energy (see Fig. 3), the parameters at other energy points should follow very closely the solid curve traced through the loci of best-fit parameters. The "errors" in the imaginary potential W_0 indicate that within this range of W_0 the χ^2 's are essentially the same (less than 5% variation in the values of best χ^2). The exceptionally high value of W at $E_p = 14$ MeV will be discussed in Sec. IV.

At each of the energy points where a parameter search was made, the angular distribution was fitted by a fine grid searching of V_0 and W_0 independently. The variation in V_0 was from 0 to 150 MeV by 2-MeV steps, and that in W was from 0 to 30 MeV by steps of 0.5 MeV. A contour map for

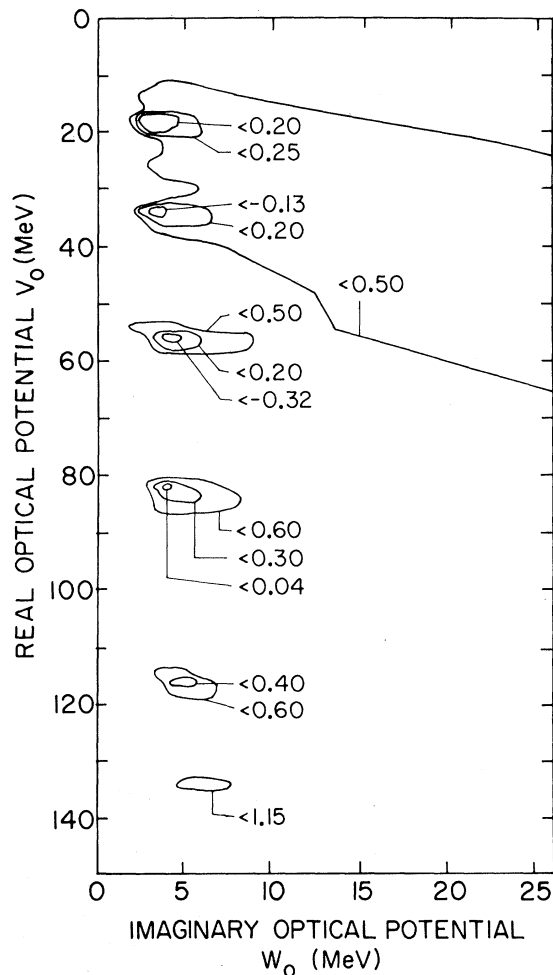


FIG. 4. Contour map of χ^2 as a function of the real and imaginary parts of the optical-model potential at $E_p = 12$ MeV. The contours contain minima in χ^2 and are labeled with values of $\log_{10}\chi^2$.

χ^2 as a function of V_0 and W_0 is obtained as illustrated by Fig. 4, the χ^2 contours of $E_p = 12$ MeV. (Contour curves are labeled by their $\log_{10}\chi^2$ values.) By inspection, the relative (or local) minima were located, and V_0 and W were again searched around these in fine grid steps.

Two real potentials about 22 MeV apart were found to give good fits at most of the energy points. For example, at $E_p = 12$ MeV (see Fig. 4), both $V_0 = 56.5$ and $V_0 = 34.0$ MeV give very excellent fits to the data ($\chi^2 < 1$ for both cases), albeit $V_0 = 56.5$ MeV gives a slightly better χ^2 . Thus, the discrete ambiguity in V_0 is not removed by scattering near the top of the barrier with a 3% error. A well depth of ~ 55 MeV gives the right number of occupied states for nucleons in ^{208}Pb . Furthermore, it is in reasonable agreement with results obtained by other investigators^{2,15,16} for proton scatterings by various nuclei in the neighborhood of $A = 208$.

The spin-orbit potential was included in the parameter search. Various choices of the spin-orbit parameters V_{so} , R_{so} , or a_{so} have essentially no effect on the computed results. For example, varying V_{so} from 0 to 20 MeV F^2 produced only about 1% changes in the χ^2 values. Because of this insensitivity, the parameters were kept constant and fixed at $R_{so} = 7.5 F$, $a_{so} = 0.65 F$, and $V_{so} = 5.0$ MeV F^2 throughout the searches of V_0 and W_0 . These values are arbitrary with respect to this analysis, but are comparable to those used by Greenlees *et al.*⁹

The best fits to the angular-distribution data are shown in Fig. 1 and the excitation functions are given in Fig. 2. In these figures, the dots are the experimental data and the solid curves represent the best fits with the optical-model parameters given in Table I. The energy dependence of the optical-model parameters is shown in Fig. 3.

Although the 3% measurement narrowed the choice of real well depths to two discretely am-

TABLE I. Best-fit optical-model parameters with fixed geometry parameters $R = R_C = R' = 7.5 F$, $a = a' = 0.65 F$. The spin-orbital potential strength is fixed at $V_{so} = 5.0$ MeV F^2 , $R_{so} = 7.5 F$, and $a_{so} = 0.65 F$.

| E_p (MeV) | V_0 (MeV) | W_0 (MeV) | χ^2 |
|----------------|----------------|----------------|----------|
| 8.0 | 59.8 | 0.8 | 1.71 |
| 9.0 | 59.3 | 2.3 | 0.67 |
| 10.2 | 57.4 | 3.2 | 0.64 |
| 11.2 | 57.0 | 3.6 | 0.60 |
| 12.0 | 56.0 | 4.2 | 0.40 |
| 12.8 | 55.0 | 4.4 | 1.10 |
| 14.0 | 53.8 | (7) | 4.4 |

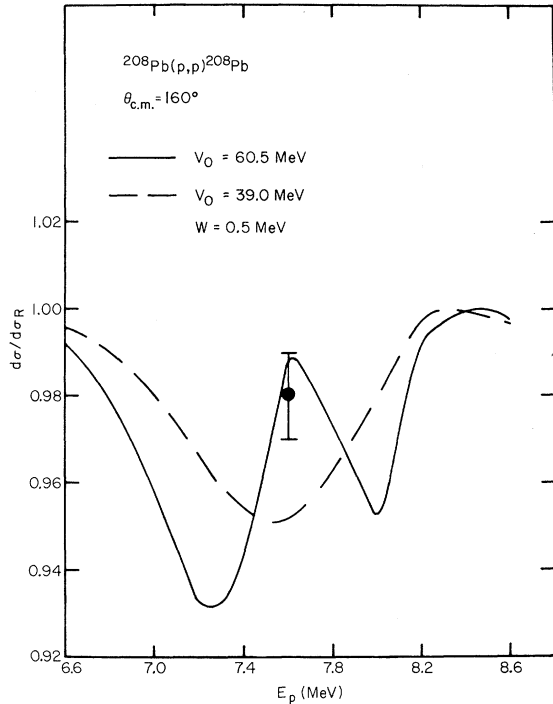


FIG. 5. Computed excitation curves for $V_0 = 39$ and $V_0 = 60.5$ MeV.

ambiguous values, a definitive selection of one potential was not obtained. Using the two sets of parameters, excitation curves were calculated to determine the bombarding energy at which the two computed curves are maximized. This obtains at 7.6 MeV, where the separation between the curves is about 3.5% (see Fig. 5).

Figure 6 shows the angular-distribution measured at 7.6-MeV proton energy for which the statistical errors are less than 1%. The solid curve is the optical-model fit with $V_0 = 60.5$ MeV and the dashed curve is that for $V_0 = 39$ MeV. With the improved precision of measurement, the choice of the deeper potential is clear.

IV. DISCUSSION

An energy dependence of optical-model parameters is necessary for reproducing the excitation

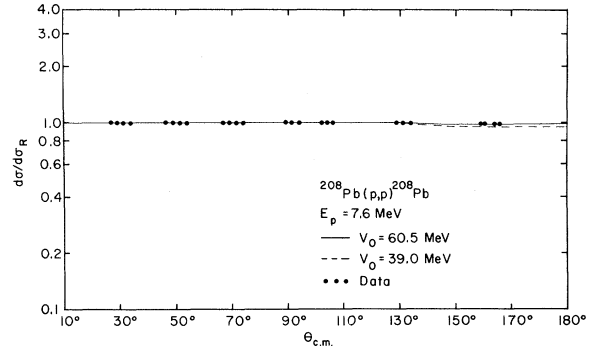


FIG. 6. Angular distribution measurements at $E_p = 7.6$ MeV with optical-model fits for $V_0 = 39$ and $V_0 = 60.5$ MeV.

functions. The variation of V_0 with E is approximately linear:

$$V_0 \approx 60 - \alpha(E - 8.0),$$

where α is ~ 0.75 . This average value of α is consistent with that for other nuclei⁸ in this energy region. As seen in Fig. 3, W increases with E , most rapidly at low energies. The value of W at $E_p = 14$ MeV (see Fig. 3) is exceptionally high. A strong isobaric-analog-state resonance^{3,4} is located at $E_p = 14.95$ MeV with a half width about 0.5 MeV. The rise in W at 14 MeV is assumed to be due to this resonance. An extrapolation of the curve ignoring this point is given by the dashed line.

The computed cross sections are insensitive to choice of spin-orbit parameters for the required values of V_0 and W_0 . The absorption potential strength damps out the fine structure due to the spin-orbit coupling. Fits to polarization data should produce more meaningful spin-orbit parameters, although this is not the conclusion found by Greenlees *et al.*⁹

ACKNOWLEDGMENTS

The authors would like to thank Dr. D. Robson and Dr. A. Adler for valuable discussions. The assistance of C. Fetrow, S. Javadi, K. Knuth, A. Zander, and M. Hudson in taking the data is gratefully acknowledged.

*Work supported in part by the Air Force Office of Scientific Research, Office of Aerospace Research, United States Air Force, under AFOSR Grant No. AF-AFOSR-69-1674, and by the National Science Foundation Grants Nos. GJ-367, GP-25974, and GU-2612.

¹G. Schrank and R. E. Pollock, Phys. Rev. **132**, B2200 (1964).

²R. M. Craig, J. C. Dore, G. W. Greenlees, J. S. Lil-

ley, and J. Lowe, Nucl. Phys. **58**, 515 (1964); B. W. Ridley and J. G. Turner, *ibid.* **58**, 497 (1964).

³C. F. Moore, L. J. Parish, P. von Brentano, and S. A. A. Zaidi, Phys. Letters **22**, 616 (1966).

⁴N. Stein, C. A. Whitten, Jr., and D. A. Bromley, Phys. Rev. Letters **20**, 113 (1968).

⁵G. M. Temmer, in *Isospin in Nuclear Physics*, edited by D. H. Wilkinson (North-Holland, Amsterdam, 1970).

⁶J. S. Eck, R. A. LaSalle, and D. Robson, *Phys. Letters* **27B**, 420 (1968).

⁷B. D. Watson, D. Robson, D. D. Tolbert, and R. H. Davis, *Phys. Rev. C* **4**, 2240 (1971).

⁸For example, see M. A. Preston, *Physics of the Nucleus* (Addison-Wesley, N.Y., 1962), p. 547.

⁹G. W. Greenlees, C. H. Poppe, J. A. Sievers, and D. L. Watson, to be published.

¹⁰K. R. Chapman, *Phys. Bull.* **20**, 415 (1969).

¹¹E. J. Feldl, P. B. Weiss, and R. H. Davis, *Nucl. Instr. Methods* **28**, 309 (1964).

¹²B. D. Watson, Ph.D. dissertation, The Florida State University, 1969 (unpublished).

¹³D. D. Kerlee, J. S. Blair, and G. W. Farwell, *Phys. Rev.* **107**, 1343 (1957).

¹⁴R. Hofstadter, *Nuclear and Nucleon Structure* (W. A. Benjamin, New York, 1963).

¹⁵D. R. Winner and R. M. Drisko, in *Phenomenological Optical-Model Parameters*, Technical Report, Sarah Mellon Scaife Radiation Laboratory, 1965 (unpublished).

¹⁶E. Rost, *Phys. Letters* **26B**, 184 (1968); H. R. Kidwai and J. R. Rook, *Nucl. Phys.* **A169**, 417 (1971).

Level Densities near $A = 200^*$

S. M. Grimes, J. D. Anderson, J. W. McClure, B. A. Pohl, and C. Wong

Lawrence Livermore Laboratory, University of California, Livermore, California 94550

(Received 9 February 1972)

Neutron spectra from the reactions $^{197}\text{Au}(p,n)^{197}\text{Hg}$, $^{209}\text{Bi}(p,n)^{209}\text{Po}$, $^{181}\text{Ta}(\alpha,n)^{184}\text{Re}$, and $^{197}\text{Au}(\alpha,n)^{200}\text{Tl}$ have been analyzed to extract the level-density parameters for the appropriate residual nuclei. Comparisons with constant-temperature and Fermi-gas forms indicate that both forms describe the data over a limited energy range. A recent calculation of the magnitude of shell effects by Gadioli *et al.* is compared with the experimentally determined values; this approach provides a better estimate of the level density of ^{209}Po than does the standard Fermi-gas model in which shell effects are included in the level-density parameter a .

I. INTRODUCTION

Although the level densities of nuclei near closed shells are known to be significantly lower than neighboring nuclei more removed from closed shells, there remains considerable uncertainty as to the appropriate functional form for the level density. One of the basic assumptions of the Fermi-gas model is that the single-particle levels are equally spaced in energy; this condition is clearly not met near closed shells. Corrections to the standard Fermi-gas form have been proposed which involve changes in the level-density parameter a ^{1,2} or shifts in the excitation energy^{3,4} to reduce the level density near closed shells.

Experimental results have not been completely consistent. Measurements of emission spectra by Maruyama,⁵ Buccino *et al.*,⁶ and Thompson⁷ have indicated that the energy dependence of the level density near closed shells is closer to a constant-temperature than a Fermi-gas form. Other experiments, including those of Mathur, Buchanan, and Morgan,⁸ Huber *et al.*,⁹ and Magda *et al.*¹⁰ have yielded agreement with the Fermi-gas model, with the closed-shell effects manifested only in reduced values of the level-density parameter a relative to nuclei farther from closed shells.

The largest and most reliable body of informa-

tion available on level densities near closed shells is that obtained from resonance counting at the neutron binding energy, and surveys^{1,11} of level-density parameters have been based in large part on these data. Because such measurements give only the absolute value of the level density at a specific energy (and even this value can be obtained only if the spin cutoff parameter is known), they do not determine the functional form of the level density. Recent measurements¹² of α emission from compound nuclei formed by α bombardment of Ta, Au, and Pb at energies of 50–80 MeV show that the Fermi-gas parameters obtained from fits to the level density at the neutron binding energy do not fit data at higher energies. It is suggested by Chenevert *et al.*¹² that the Fermi-gas parameters which fit level densities at excitation energies of 40 MeV have essentially no remaining shell effects; i.e., the influence of shell closures must be confined to energies somewhat less than this.

Gadioli *et al.*¹³ have calculated the effect of the closed shells at $Z = 82$ and $N = 126$ on the level densities of nuclei near ^{208}Pb . Their results yield a functional form only for the level density of ^{208}Pb itself, but the effects on level-density parameters for neighboring nuclei can at least be estimated. The results obtained by Gadioli *et al.* are similar